A liquid interaction with ultrahydrophobic surfaces

Darina Jasikova[1,a], Michal Kotek[1], Simona Fialova[2] and Vaclav Kopecky[1]

[1] *Department of Physical Measurement, Technical University of Liberec, The Institute for Nanomaterials, Advanced Technology and Innovation, Studentska 1402/2 Liberec 1 461 17, Czech Republic*

[2] *Faculty of mechanical engineering, Brno University of Technology, Technicka 2896/0, Kralovo Pole, 61669, Brno, Czech Republic*

Abstract. The interaction of the liquid with ultra-hydrophobic surfaces was so far studied through estimation of static contact angles. It appears now that this interaction is more complex, and cannot be described only with static methods. Effect of ultra-hydrophobic surfaces and their advantages are also particularly in dynamic interaction with liquids. One of the parameters that determine the character of the dynamic interaction is presence of air film close to the surface. The thickness of air film can be measured with long distance microscopy and the interaction with the flow using micro PIV method. Here we present the results of measurements of the air film that is created close to ultra-hydrophobic surfaces and the dependence of its thickness on the Re number.

1 Introduction

The effect of the surface roughness on the skin friction is well known. There are not explored enough interactions between chemically modified surfaces and liquids. First, because the development of new surfaces is based on the influence of surface energy using cold plasma technique and applying special chemical structures. In any event, such surfaces macroscopically appear as ultra-hydrophobic (UH) and provide their use specifically in the interaction with liquids, i.e. in hydraulic machines, or a pipe system. It is expected that the change of the static contact angle (CA>150°) is reflected in the dynamic properties, e.g. skin friction coefficient and reduction of hydraulic losses.

Dynamic interaction of the liquid with UH surface is accompanied by formation of a layer of air film. The parameters and the quality of the air film are dependent on the quality and uniformity of UH surface and also its roughness, which results from the basic characteristics of skin friction.

Although, there were already published theoretical works on mechanism of air layer, there has not been presented satisfactory experimental evidence yet. [1]

The motivation of this project is the visualization of air film and its quantitative description. There has been compiled methodology and principles based on micro PIV and long distance microscopy methods as part of this project.

2 Experimental facilities

The UH surface is commonly coated on boards or entire blocks. Here there was manufactured the channel

that should followed the requirement of the visualization methods.

Manufacturing of experimental facilities belongs to the one of research itself. It's a sector as important as the compilation of measurement technology and design of fluid section. There was designed a channel made from the modification of plastics (PCBs, PVC, PA) and traditionally manufactured by segments bonding.

Individual parts were designed so channel assembly was created (mini-channel) with dimensions of width w = 5 mm, height h = 3 mm, and functional length l = 150 mm.

Each part of the channel was accurately machined and edges polished for a defined roughness Ra of 0.5 micron. Furthermore, parts were glued together as it is seen on figure 1.
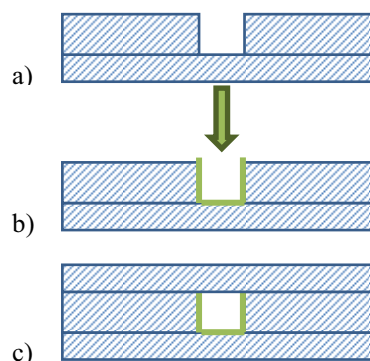

Figure 1. Process of manufacture of the mini-channel: A) opened channel prepared for the surface treatment procedure, B) surface treatment, C) closing the channel with the optically clear and untreated surface.

The inner surface of the mini-channel was treated with UH surface in cooperation with Masaryk University

[a] Corresponding author: darina.jasikova@tul.cz

of Brno. Before the completion of the experimental facility, the surface roughness and static contact angle was measured.
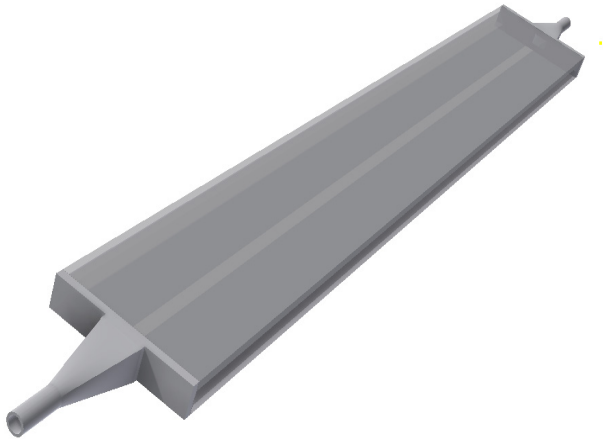

Figure 2. Construction of segments, their completion and set up with the joining reductions connected with the rest of hydraulic circuit.

The channel had the rectangular profile, so it was fitted with interfaces from circular to rectangular section for additional connection with hoses. The interfaces were designed in CAD software and produced by Rapid Prototyping - 3D printing technique. Connections were made of Vero White material, i.e. cross linked UV photopolymer used in 3D printers. The jumpers were optimized for Luer-lock connection system and a standard hose (6x4) mm.

3 Visualization techniques

The visualization of the air film came out from the micro PIV measurement technique. This technique allows the visualization, tracking and evaluation processes within a very small scale of nanometres to micrometres. The design of the measurement track and the samples were adapted to his method.

The micro PIV technique provided us the information about the air film thickness. This technique was suitable for studying small area of interest, such as 1,5mm. We used the long distance microscopy to cover the whole velocity profile across the channel – 5mm.

The basis of micro PIV technique is a laser beam, which illuminates the entire volume of the examined space. The investigated volume of liquid is enlarged with an inverted microscope, which is equipped with a magnifying lens. The magnifying lens also ensures the depth of field. The Technical university of Liberec is equipped with micro PIV system that is based on an inverted microscope Leica DMIL and fitted with a set of lenses: 5x, 10x, 20x and 50x. For illumination of the evaluated area NewWave Gemini pulsed laser is used Nd: YAG type, energy of 120mJ per pulse length of 10ns, wavelength 532nm.

The images are captured with Neo CMOS chip 5,5MPixel size of 6.5 microns camera. Laser and camera system is controlled from a computer and synchronized with the external TimerBox.

Unlike standard PIV method, where the depth of field depends on the distance to the measurement object from the camera lens, f-number, in the micro PIV method depth of field is dependent on the parameters of the microscope lens, index of refraction of the liquid, and the wavelength of used light. Other parameters are related to the system of lenses: NA - iris, M - total magnification microscope, and e - the distance between the pixels on the CCD camera.

The depth of field is calculated using the relation (1). The arrangement of micro PIV has a constant depth of field 4um at 10x magnification. This factor is important for choosing the size of seeding particles. Here in this investigating we used coated Rhodamine B 2 µm fluorescent particles.

$$\delta = \frac{n\lambda}{NA^2} + \frac{n.e}{NA.M} \qquad (1)$$

We used set of microscopic calibration targets for the calibration of the system to determine the magnitude coefficient. At 5x magnification dimensional coefficient was set at 0.1999 and at 10x magnification was set at 0.0998. The records of calibration grid also allow creating an image for further image dewarping to eliminate the image distortion. The figure 3 shows the calibration target with 50 µm grid.
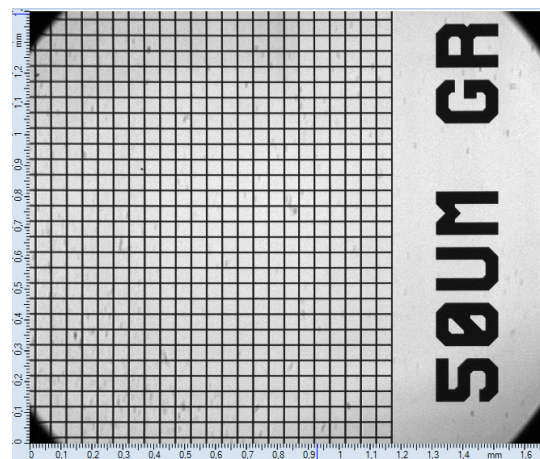

Figure 3. The example of the calibration target optimal for the magnification 10x.

The long distance microscopy method was used for the measurement of the velocity profile over the whole channel in one step. This optical setup was based on INFINIPROBE™ TS-160 universal macro/micro imaging system that enables 4x and 16x magnification. This probe was working in the set of compressor for the wide field of view, and the working distance was 100mm in the macro regime. The area of interest was illuminated with the laser light led with optical cable towards the sample.

The measurements run at 12Hz frequency with 60mW laser power at one flash. The light from the laser head was brought to the microscope lens system with optical cable. For each measurement at least 290 records were always acquired and were further processed by the

correlation function, validation and filtering before being evaluated statistics and estimated velocity profiles.

4 Testing section

The assembling of hydraulic circuit went from lab equipment and requirements of the visualization technique on the organization of the experiment.

The investigation of the interaction between hydrophobic surfaces and liquids was run under Re number in laminar, transient and turbulent zone. Following this requirements we used Micropump gear pump. The advantage is almost zero slip, accurate dosing and zero pulsation. Faultless operation of the pump pulsation has been assessed by measurement. Pump speed was controlled by the applied voltage. The system was therefore enhanced with a linear precision voltage source KORADO KA3005P controllable from a PC and an adjustable voltage with an accuracy of hundredths. The flow was measured by the flowmeter FL 1440 to ensure the repeatability of measurement. The dependence of voltage, flow, and consequently Re numbers were necessary to provide for the conversion table.

Re number was determined according to the equation 2 and 3.

$$D = \frac{4A}{P} = \frac{4wh}{2w+2h} \qquad (2)$$

$$Re = \frac{uD}{v} \quad , \qquad (3)$$

where u is the mean velocity on the outlet, D hydraulic parameter, and v is kinematic viscosity of water $(1,004.10^{-6}$ at 20 °C). Characteristic hydraulic parameter of the mini channel is 3,75 mm. The calculation of the Re number was performed for the channel without the surface treatment, so the effect of the air film was neglected.

5 Results and discussion

5.1 The preparation of the samples

The inner walls of channel were treated with three different methods on polypropylene and polycarbonate to create UH deposited layer.

The sample A was spray coated with nanopolymeric UltraEverDry®, UED® in two layer was applied on the sample B and the sample C was continuously sprayed with UED® and cold Ar+O$_2$ plasma treated [4].

Surface roughness was measured before the channel chemical treatment of the inner surface and it was 0,5um. This surface roughness correspond to static contact angle 110°. We used the touch laboratory device Mitutoyo Surftest SV-2000 for the surface roughness estimation and it was measured and averaged over 100 mm. The average roughness of the treated surface sample A increased to 0,8 μm, on the sample B it increased to 1,5 μm, and on the sample C roughness increased to 0,9 μm.

The global increase of the surface roughness can be explained due the UED® nanoparticles coagulation during the process, as it is seen in figure 4. The surface roughness has the direct effect on the static contact angle: the surface on the sample A had the CA 150°, sample B 160°and the sample C 150°. Wet surface was also measured, but the changes in static contact angle were not significant. All measurements were also done on the reference sample. The reference sample was left untreated.
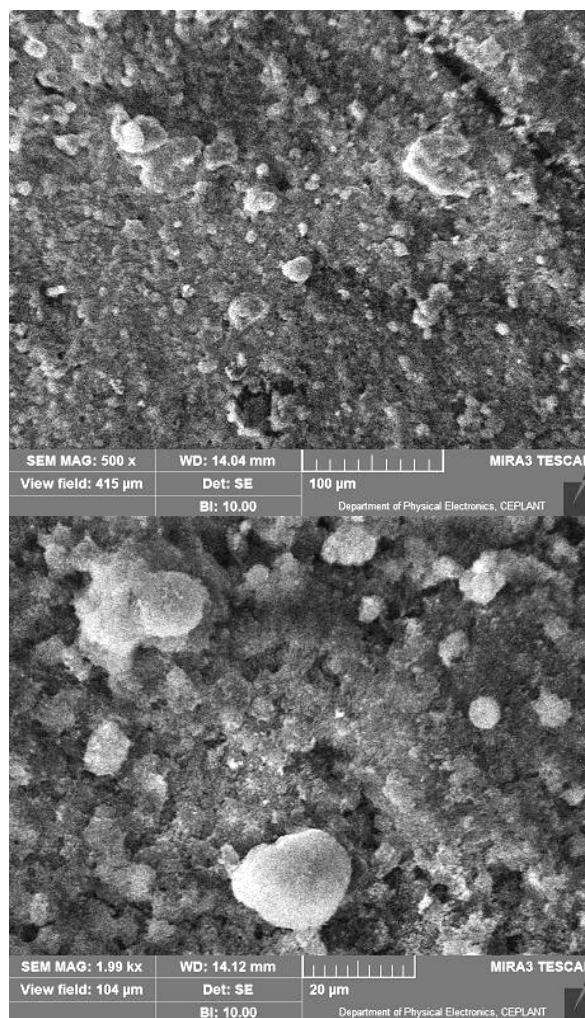

Figure 4. The treated surface UltraEverDry® under SEM microscope, magnification of 500x and 2000x.

5.2 Estimation of air film

The character of the air film comes from the principles of manufacturing of samples. There are three walls treated and the one that creates the cover is left clean. This clear wall allows optical access for the visualization and measurement.

Here we worked with distilled water. It is supposed that water contains certain amount of dissolved inert gases and micro-bubbles. The whole amount of present gas in water was 8 mg O$_2$/l at 20 °C. This value was measured with laboratory oximeter. There can be estimated total dissolved gas in the water with the knowledge of concentration of oxygen in air. The concentration of the dissolved air and amount of bubbles

is strongly dependant on the partial pressure. It is said that degassed water contains about $0,911\times10^{9}$ nucleus of most probable size about 6 μm. [1]

Basically the growth of dissolved air on the surface can be divided into three categories: the first describe the situation, when the dissolved air is due the diffusion entrapped on the surface as the unique bubbles. These bubbles are said to be initialized in the turbulence layer in seeds. The seeds can be caused by local roughness, impurities or local change in pressure/density gradient. The growth of these single bubbles is time dependent and could grow up to 1,5 mm. Then these bubbles are changing character of the boundary layer and, of course, they active react on local pressure changes that lead to pulsations.
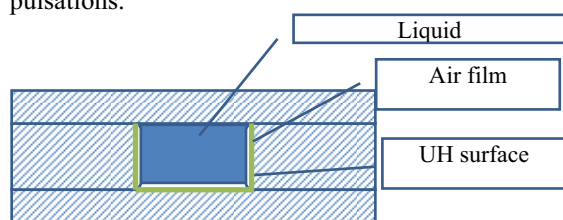

Figure 5. The geometry of the air film formation in the mini-channel.

In the second category the dissolved air is formed into more or less uniform air film. The formation of the air film is dependent on the flow pattern. This flow pattern is stratified into film–gas interface and could finally lead to multi-phase flow. The film structure is dependent on the geometry of the channel, roughness of the surface and it can be symmetrical or unsymmetrical.
It is said, that the air film thickness is dependant mostly on the channel geometry, that is represented by the hydraulic parameter D and α the amount of the dissolved air, so we can estimate the relation:

$$d=D(1-\sqrt{1-\alpha})/2 \qquad (4)$$

, but according to previous formulation, that the air film is dependent on the flow pattern, this can be expressed using Re number.
Following this formulation the interaction of the liquid flow and the air film can be divided into two regions: Re<500, and Re>500. In the first are acting macroscopic eddies instead of the second one with microscopic eddies. Anyway, here the interaction moved from the liquid/surface to gas/liquid interface.

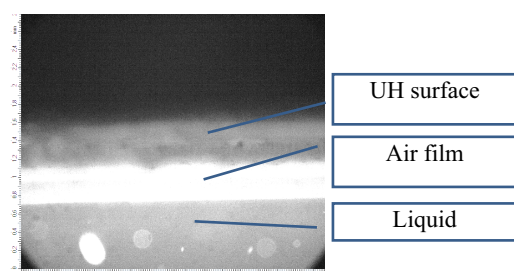In the third category of formation of dissolved air, it overgrows the channel geometry and aerates the channel.

Figure 6. The visualization of the air film with the microscope magnification 10x.
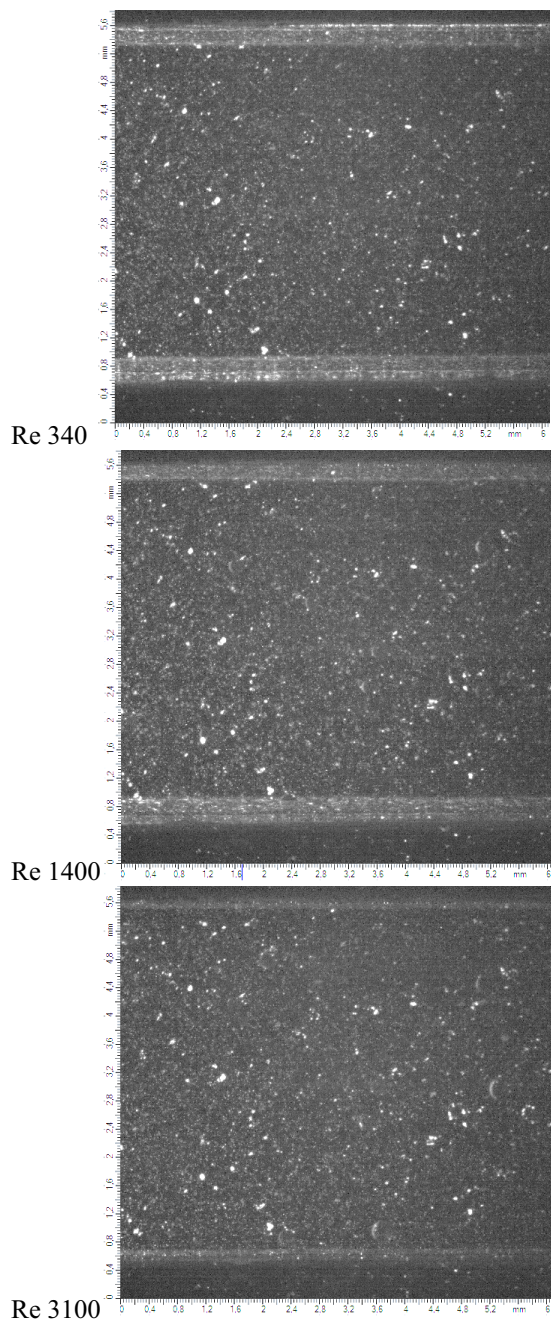

Re 340

Re 1400

Re 3100

Figure 7. The visualization of the air film on the sample A – the situation in the whole channel. There are three examples selected: Re 340, Re 1400 and Re 3100.

This theoretical description of the existence of the air film on the UH surfaces had to be firstly proved its existence and demonstrated with the visualization technique. This would allow further description of the effect.
The existence of the air film formation was proved with microscopic view. The film is formed in the region Re<500 and can be seen as light stripe that reflects the light. This stripe narrows in dependence on the Re number, respectively of the flow velocity. The visualization of the air film is seen in figure 6.
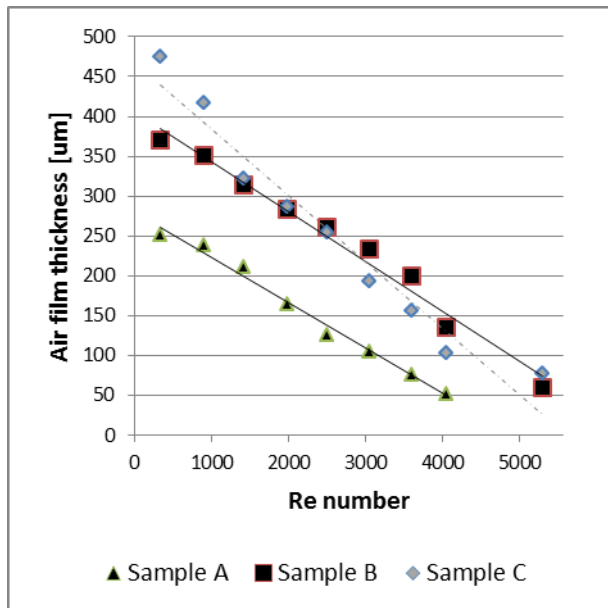
Figure 8. The graph: air film thickness dependant on Re number.

The microscopic view proved the local existence of the air film, but we were interested in the situation in the whole channel geometry. For this study we used the long distance microscopy setup. Figure 7 shows the complex situation of the air film formation depending on the Re number. There could be seen the decrease of the film thickness, when Ren number exceed the value for transient zone. The air film completely extinguished with high Re numbers.

Conclusiveness of this visualization was validated with the fluorescent method. The water was coloured with fluorescence dye (Rhodamine 6G), that is concentration sensitive and the air film was visualized in the green laser light (532 nm) for the excitation. The emitted light gave us information about local concentration and the relation between water and gas. The air film was seen as a very dark region. This means there was no concentration of the fluorescent dye in this layer.

5.3 The effect of air film on velocity profile

After this proof of the existence of symmetrical air layer with two different methods, that were repeatable, we studied the effect of the air film on the character of the velocity profile [5].
In the first step the velocity profile was measured. The air layer reduces the lumen cross section, resulting in maintaining a constant speed of the pump it leads to increase of the maximum velocity in the flow profile. The maximal differences could be seen in laminar zone. The thickness of air film for Re 340 reaches for sample A 250 μm that reduces the lumen cross section to 82%, for sample B 360 μm, that means 75%, and for sample C the air film thickness is 470 μm, so the reduces are to 68% of full cross section area. This corresponds with the maximal velocity that is seen in figure 9. There is added velocity profile for reference sample in figure 9, 10, and 11. This reference sample was untreated polycarbonate

channel with (5x3) mm cross section. The velocity profiles were taken over the whole cross section and respect the air film on the boundaries. The profiles were analysed from the statistics that contained 290 dataset of vector maps taken with frequency 12Hz.
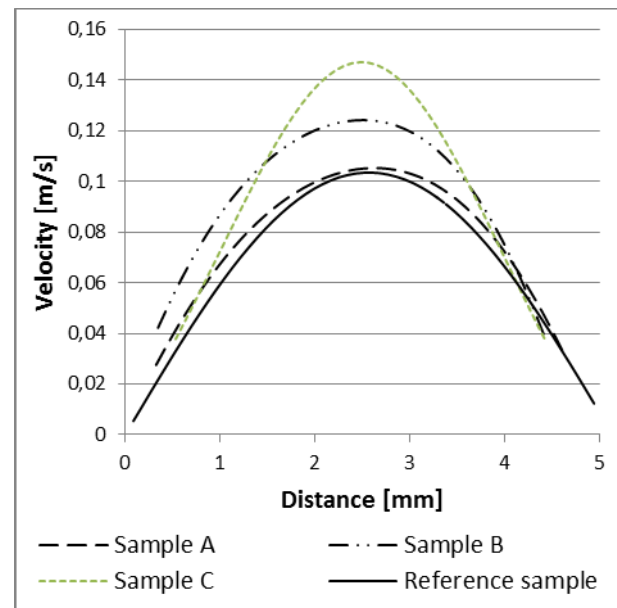

Figure 9. The chart of the velocity profiles for samples A, B, and C for Re 340.

In the figure 10 there is seen the situation of the velocity profile for the Re number 1400 that supoosed to be in the transient zone. There is significant decrease of velocity in the middle of the channel. This effect is caused by the increases of micro eddies in the middle of the cross section. The air film thickness for sample A was 200 μm, for sample B 314 μm and for sample C it was measured 322 μm. The effect of decrease of cross section area due the air film is not so significant and more reduce the transition on the boundaries close to the surface [2, 3].
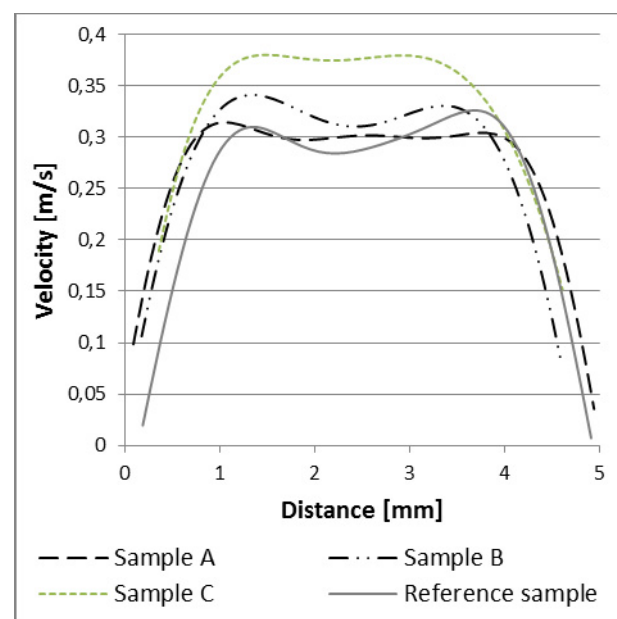

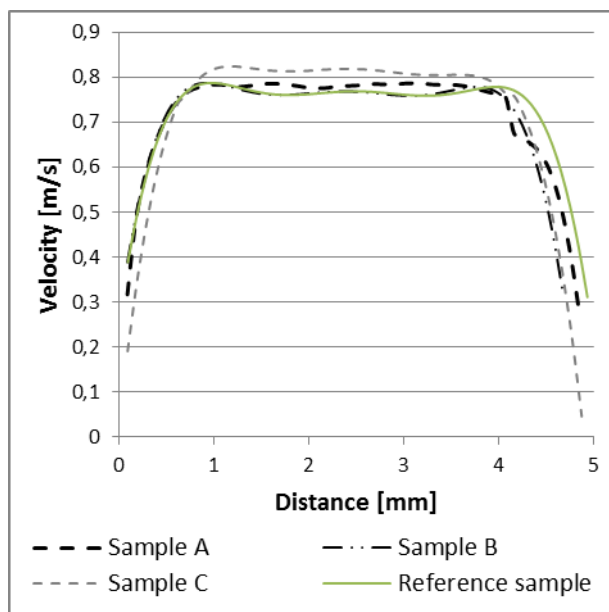**Figure 10.** The chart of the velocity profiles for samples A, and C for Re 1400.

Figure 11. The chart of the velocity profiles for samples A, B, and C for Re 3100.

The figure 11 shows the chart of velocity profile for Re 3100 that is supposed to be in higher edge of transient zone. The air film disappears with the higher Re numbers. For Re 3100 the air film thickness reached round 50 µm for all samples. There is supposed to be no air film for the Re number in turbulence zone, for Re > 4000. For high Re number the surface structure is fully wet and the pores are filled with water. When this happens, there is no recovery of air film over the surface, even if the water flow stops. The measurement of the static contact angle proved the decrease of 20° and more, on the fully wet surface. This corresponds with nonexistence of air film on the surface that reach static contact angle round 110°. This value of static contact angle was typical for the untreated reference sample. The ultra-hydrophobicity can be restored after deep drying of the surface. Testing how many cycles' surface withstands (full wetting and drying) may be a novel method that will test the quality of the UH surface dynamic test. In this study all samples were strained three times and the result were comparable, this means there were no significant changes in the structure that would negatively influence its quality.

6 Conclusions

Dynamic interaction of the liquid with UH surface is accompanied by formation of a layer of air film. The proof of the quality of air film belongs to one of dynamic characteristics of ultra-hydrophobic surfaces. So far, the ultra-hydrophobic surfaces were described only by static method, measuring contact angle. However, sometimes the UH surfaces are not achieve the expected behaviour in the dynamic interaction with liquids, although their CA is higher than 150°. The parameters and the quality of the air film are dependent on the quality and uniformity of UH surface and also its roughness, which results from the basic characteristics of skin friction. The quality of the surface can be studied with microscope. Here we set

the method to explore the quality of the air film depending on the surface roughness and the Re number. This relationship is mutual according to the results. As the dynamics of fluid flow is acting on the air film, the air film is influencing the character of liquid interaction as well as the maximal velocity of the flow. The qualities of UH surface are shown as the flow velocity is kept in transient area of Re number. In any event, the knowledge of this phenomenon and the way how it affects the flow expands the awareness of the dynamic interaction between the UH surfaces and liquids and has to be taken in account in the mathematical descriptions.

Acknowledgements

References

1. Nikolay I. Kolev, *Multiphase Flow Dynamics 3*, (Springer-Verlag Berlin Heidelberg, 2007)
2. Ch. J. Kahler, S.Scharnowski, Ch. Cierpka, Exp. Fluds, **52** (2012)
3. V. K. Natrajan, K.T. Christense, Microfluid Nanofluid, **9** (2010)
4. M. Klíma, etal., *Method of realisation of polyreactions, plasma-chemical polyreactions, their modification and modification of macromolecular substances by the plasma jet with a dielectric capillary enlaced by a hollow cathode*, EP 07466017, (2007)
5. F. Pochyly, et. al, International Journal of Fluid Machinery and Systems **3** (2010)